



OPEN Anti-diabetes activity of (*R*)-gentiandiol in KK^{Ay} type 2 mice

Yaqi Xu¹, Jinyue Huang¹, Shuhan Tang^{2,3}, Yidan Sun¹, Hao Li¹, Pengyu Li¹, Xianna Li¹, Masao Hattori², Xiuhong Wu¹, Hailong Zhang⁴ & Zhigang Wang^{1,2}✉

Swertiamarin is a major component of many traditional Chinese *Swertia* herbs that show significant antidiabetic activity. (*R*)-Gentiandiol and (*S*)-gentiandiol are metabolites of swertiamarin found in vivo. The antidiabetic activity of swertiamarin and its nitrogen-containing metabolites (*R*)-gentiandiol and (*S*)-gentiandiol was evaluated in this research, and their mechanism of action was investigated after evaluating the serum metabolic profile of KK/Upj-*Ay* type 2 mice. The pharmaceutical effects of swertiamarin, (*R*)-gentiandiol, and (*S*)-gentiandiol were tested by biochemical indices and histopathological observations. Moreover, the mechanism underlying the action of three compounds against type 2 diabetes was elucidated using a metabolomic method. It was shown that (*R*)-gentiandiol significantly improved pathological changes in the kidney and pancreas. The levels of total cholesterol, triglyceride, and high-density and low-density lipoprotein cholesterol improved considerably after treatment with (*R*)-gentiandiol, compared to their levels in model mice. However, the levels of these compounds showed no improvement after treatment with (*S*)-gentiandiol. In total, 15 biomarkers were identified in KK/Upj-*Ay* type 2 mice, and the levels of 10 biomarkers were measured after treatment with (*R*)-gentiandiol. (*R*)-Gentiandiol reduced the abnormalities in metabolic pathways, including lipid metabolism, amino acid metabolism, carbohydrate metabolism, and nucleotide metabolism. Additionally, glycine, serine, and threonine metabolism related to the regulation of glycine was affected the most. The study indicated that the antidiabetic effects of *Swertia* herbs may due to (*R*)-gentiandiol which is a metabolite of swertiamarin in vivo. This study helps clarify the active metabolites of swertiamarin, provide greater insights into the clinical antidiabetic effects of *Swertia* herbs and bring novel ideas for developing new drugs from antidiabetic herbs.

Keywords Swertiamarin, (*R*)-Gentiandiol, Type 2 diabetes mellitus

Type 2 diabetes (T2D) is a chronic heterogeneous metabolic disorder¹. According to the IDF Diabetes Atlas (10th Edition), the incidence of T2D is ever-increasing around the world, which has caused diabetes to be labeled as a major global threat to the well-being and health of patients, their families, and society. Reports suggest that 537 million people (aged 20–79 years) worldwide are living with T2D². T2D is among the top 10 factors leading to mortality worldwide; the global death toll due to diabetes increased by 70% between 2000 and 2019³. T2D is characterized by an increase in blood glucose levels resulting from unresponsive pancreatic insulin secretion and insulin activity⁴. T2D is caused by multiple factors and is associated with genetic factors and environmental conditions. However, its incidence among children and adults has increased because of obesity, insufficient nutrition, and a sedentary lifestyle⁵. Additionally, T2D can cause various complications, including retinopathy, nephropathy, angiocardopathy, and residual foot problems^{6–9}. T2D is also associated with various metabolic abnormalities, with metabolic alterations being its central mechanism.

Therefore, effective analytical methods are needed to detect metabolic biomarkers for the development and treatment of T2D. Metabolomics is a discipline that takes a holistic approach, allowing the analysis of metabolites at the metabolomic scale and a holistic view of overall metabolism¹⁰. Among them, non-targeted metabolomics provides a complete metabolic analysis for biological systems to screen candidate biomarkers that have high sensitivity to disease and are associated with alterations. Mass spectrometry (MS) and nuclear magnetic resonance (NMR) are the foundations of metabolomics for qualitative or quantitative analysis. As MS is a highly sensitive and selective analytical approach, it can be used to effectively analyze metabolites within mixed samples, such as biological samples¹¹. Metabolomics can be used to predict and diagnose T2D early.

¹Department of Pharmaceutical Analysis, College of Pharmacy, Heilongjiang University of Chinese Medicine, Heping road 24, Harbin 150040, China. ²Institute of Natural Medicine, University of Toyama, 2630 Sugitani, Toyama 930–0194, Japan. ³Heilongjiang Hospital, Beijing Children's Hospital, Youyi road 57, Harbin 150000, China. ⁴School of Pharmacy, Health Science Center, Xi'an Jiaotong University, Xi'an, Shaanxi 710061, China. ✉email: wangzhigang0513@vip.163.com

Many researchers have used metabolomics technology to analyze and study the changes in metabolites in T2D patients to identify potential biomarkers and related metabolic pathways. Meanwhile, metabolomics technology can provide a theoretical basis for the pathogenesis of T2D¹².

Swertiamarin (ST, Fig. 1), an iridoid glycoside, is the main active ingredient in many antidiabetic *Swertia* herbs, such as *Swertia pseudochinensis* and *Swertia chirata*¹³. Iridoids such as swertiamarin, loganic acid, and gentiopicroside are the main effective components of antidiabetic *Swertia* herbs, and ST has the highest content in these herbs. Studies have shown that ST exhibits antidiabetic activity¹⁴. Although ST was found to exert its antidiabetic effect in vitro via gentianine (Fig. 1), a metabolite of ST¹⁵, the bioactive antidiabetic metabolites in vivo have not been identified. We speculated that the antidiabetic mechanism may be related to its metabolites *in vivo*. We found that gentianine could not be detected after oral administration of ST to rats because gentianine can be rapidly metabolized in vivo to two nitrogen-containing enantiomeric metabolites, (*R*)-gentiandiol (GTR, Fig. 1) and (*S*)-gentiandiol (GTS, Fig. 1), by liver P₄₅₀¹⁶. However, studies on the antidiabetic activity of GTR and GTS are lacking. This was the first study to evaluate the antidiabetic effects of ST, GTR, and GTS on KK/Upj-A^y (KKAy) type 2 diabetic mice using a non-targeted metabolomics method by UPLC-Q/TOF-MS. The effects of ST, GTR, and GTS on the regulation of serum biomarkers in KKAy type 2 diabetic mice were investigated, and the metabolic pathways related to the antidiabetic mechanisms were identified. This study revealed the active metabolites of ST and improved our understanding of the antidiabetic effects of *Swertia* herbs. Our findings can provide novel ideas for developing new drugs for treating diabetes.

Materials and methods

Instrument

An Acquity™ UPLC system (Waters, USA), Synapt™ G2 Q-TOF mass spectrometer (Waters, USA), an ultrasonic cleaner (KQ-500DB, Kunshan, China), a microplate reader (Bio Tek, USA), a table centrifuge (Thermo Scientific, USA), and a fully automatic temperature control-type high-precision polarimeter (Rudolph Research Analytical, USA) were used in this study.

Chemicals and reagents

Acetonitrile (HPLC grade) was purchased from Fisher Scientific Corporation (Waltham, USA); methanol (HPLC grade) was purchased from DIKMA Technology (Beijing, China); formic acid (HPLC grade) was purchased from Tianjin Reagent Company (Tianjin, Beijing); ultrapure water was provided by Wahaha Group Co., Ltd. (Hangzhou, China). Total cholesterol (TC), triacylglycerol (TG), high-density lipoprotein cholesterol (HDL-C),

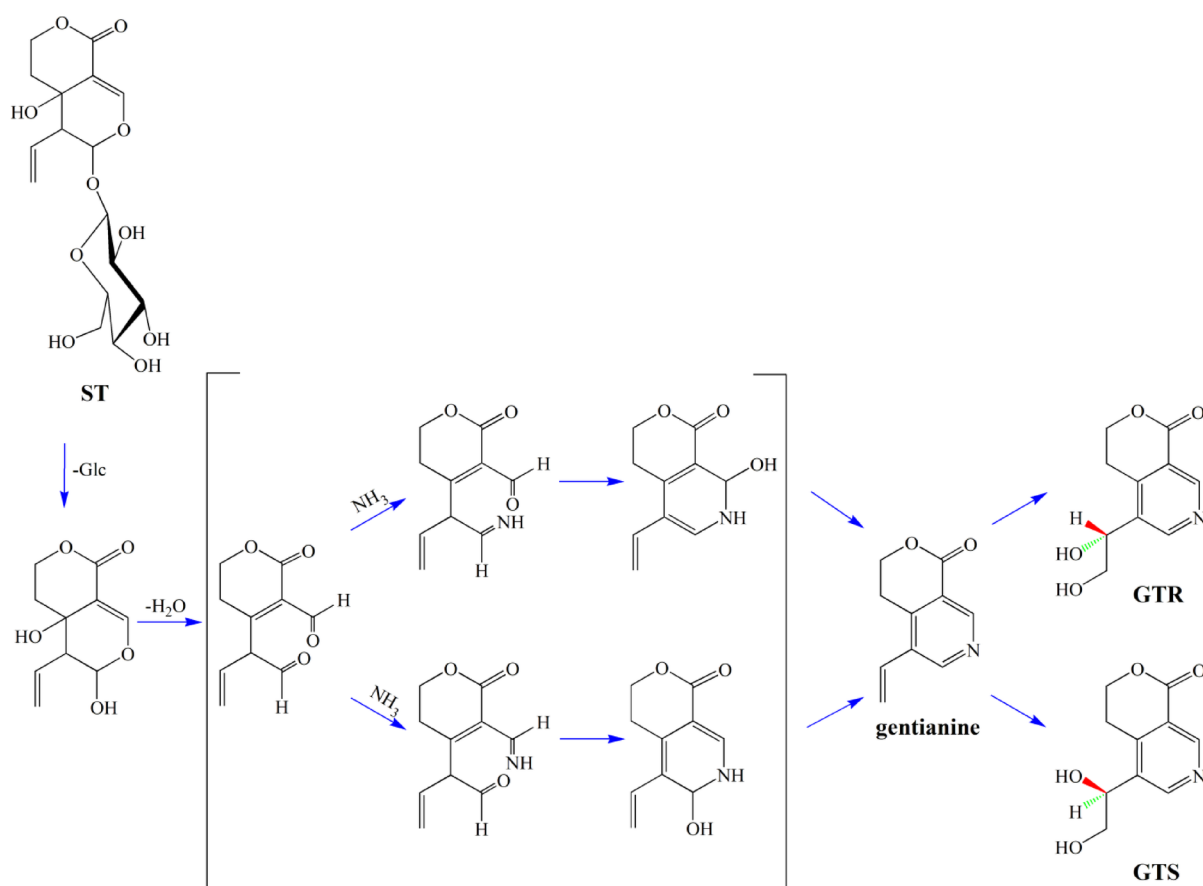


Fig. 1. Metabolic pathways for the conversion of ST to nitrogen-containing metabolites GTR and GTS in vivo.

and low-density lipoprotein cholesterol (LDL-C) assay kits were purchased from HUIJIA Bio-Technology & Science, Inc. (Xiamen, China). Swertiamarin was isolated from *S. pseudochinensis*, and GTR and GTS were synthesized from swertiamarin in our laboratory following our previously reported methods¹⁶. Metformin (Met) was purchased from Sino-American Shanghai Squibb Pharmaceutical Co., Ltd. (Shanghai, China).

Animals and sample collection

Male KKAY mice ($n=70$; 6 weeks old) and male C57BL/6J mice ($n=10$; 6 weeks old) were provided by Beijing HuaFuKang Bioscience Co., Ltd., China (No. SCXK (Jing) 2019-0008). All mice were provided access to water and food under standard laboratory conditions (temperature: 20–22 °C; humidity: 55 ± 5%; 12-h/12-h light/dark cycles). KKAY mice were fed an HFD (High-Fat Diet) (KK Diet 1K65) provided by Beijing HuaFuKang Bioscience Co., Ltd., China, and C57BL/6J mice were administered a regular diet provided by Liaoning ChangSheng Bioscience Co., Ltd., China. All animals were randomized into eight groups, including the control group (C57BL/6J mice, $n=10$), model group (KKAY mice, $n=10$), ST group (KKAY mice, $n=10$), GTR high-dose group (GTRH) (KKAY mice, $n=10$), GTR medium-dose group (GTRM) (KKAY mice, $n=10$), GTR low-dose group (GTRL) (KKAY mice, $n=10$), GTS group (KKAY mice, $n=10$), and Met group (KKAY mice, $n=10$).

KKAY mice were fed an HFD for 2 weeks, those whose random blood glucose levels were > 13.9 mmol/L were used as diabetic models. For animal treatment, GTR and GTS were dissolved in 0.9% saline and stored at 4 °C until use. From the third week, the mice in the GTRH and GTS groups were treated with 6.00 mg/kg solutions via tail vein injection; the mice in the GTRM and GTRL groups were treated with 3.00 and 1.50 mg/kg solutions via tail vein injection, and those in the ST and Met groups were treated with doses of 0.0260 g/kg and 0.250 g/kg daily, respectively, by oral administration for 7 days. The model and control groups were administered 0.9% saline (10 mL/kg) for 7 days. Fasting blood glucose (FBG) and body weight (BW) were measured 12 h after fasting, before the end of the experiment. At the end of the experiment, the mice were fasted overnight (mice were provided only water) and euthanized by cervical dislocation after being anesthetized with isoflurane gas to minimize pain. Subsequently, the serum, pancreas and kidneys were dissected and removed.

Mouse blood was maintained for 30 min at ambient temperature, followed by 10 min of centrifugation at 4000 r/min at 4 °C to separate the serum and blood cells. Next, 5 µL of each serum sample was taken and mixed to obtain a quality control (QC) sample. Finally, QC sample and other serum samples were stored at -80 °C before analysis. The experimental protocol was approved by the Ethics Committee of Heilongjiang University of Chinese Medicine (resolution No. 2023032702). This study was conducted in compliance with the ARRIVE guidelines. This study complied with the Regulations on the Management of Laboratory Animals, as issued by the National Science and Technology Commission. The conditions of the staff and the equipment were in accordance with the relevant statutes of the Experimental Animal Ethics Committee of the Heilongjiang University of Chinese Medicine.

Biochemical assays

The contents of TC, TG, HDL-C, and LDL-C in serum were analyzed using an autobiochemical analyzer (7150, Hitachi, Japan) following specific instructions.

Histopathology examination

Kidney and pancreas samples were fixed (10% neutral buffered formalin), embedded (paraffin), sectioned, subjected to hematoxylin-eosin (HE) staining, and observed under a light microscope (200x magnification).

Pretreatment of serum samples for metabolomics

Before analysis, the frozen serum samples were thawed at 4 °C. Next, 100 µL of serum was diluted with methanol (100%, 4 °C) at a ratio of 1:3 (v/v), vortexed for 60 s, and incubated for 30 min at 4 °C. After incubation, the contents were centrifuged at 13,000 rpm and 4 °C for 15 min. After the supernatants were separated and collected, they were screened with a 0.22-µm filter membrane for UPLC-Q/TOF-MS analysis.

Chromatography conditions

Chromatographic separation was performed using an Acquity™ UPLC system (Waters, USA) with a Waters UPLC BEH C₁₈ column (2.1 mm×100 mm, 1.7 µm). The samples (5 µL) were separated at a column temperature of 35 °C and an optimal flow rate of 0.4 mL/min. All samples were maintained at 4 °C. The mobile phases containing 0.1% formic acid in acetonitrile (solvent A) and 0.1% formic acid in water (solvent B) were as follows: 0–2 min, 5–50% A; 2–9 min, 50–90% A; 9–10 min, 90% A; 10–10.1 min, 90–5% A; and 10.1–13 min, 5% A.

Mass spectrometry

A Synapt™ G2 Q-TOF mass spectrometer (Waters, USA) system was used to collect mass information with an electrospray ionization (ESI) source in the both positive and negative modes. The ion capillary voltage floating was 2.6 kV; the ion source temperature was 110 °C; the ion cone voltage and gas flow were 35 V and 50 L/h, respectively; the ion desolvation temperature and gas flow were 400 °C and 700 L/h, respectively. The mass range was 50–1200 Da. The collision voltages were 4.0 and 20–40 eV for the low-energy and high-energy scans, respectively. An external standard correction (Lock-Spray™) method was used to correct the MS and MS/MS data automatically.

Data analysis

Raw UPLC-MS spectral data, including retention time (Rt), mass range, mass tolerance, and noise removal level, were obtained using MarkerLynx application manager version 4.1 (Waters, USA). These data were then input into Progenesis QI software (Waters, USA) for peak picking, alignment, normalization, and multivariate

regression analysis using the SIMCA-P (V.14.0) software. Supervised orthogonal partial least-squares discrimination analysis (OPLS-DA) and unsupervised principal component analysis (PCA) were performed to observe the distribution between groups. The model group could be distinguished from the control group ($VIP > 1$) through OPLS-DA, with the compounds with P -values (Student's t -test) less than 0.05 considered to be differential metabolites. The experimental data are presented as the mean \pm SD. Statistical analysis was performed using GraphPad Prism 9.5.1 (La Jolla, CA, USA). Data comparisons between the two groups were compared using a student's t -test. Data comparisons between multiple groups were performed using one-way analysis of variance (ANOVA) with Dunnett's multiple comparison test. The MS^E data and secondary fragment information were subsequently analyzed using the Human Metabolome Database (HMDB, <https://hmdb.ca/>). Finally, the Kyoto Encyclopedia of Genes and Genomes database (KEGG, <https://www.genome.jp/kegg/>) was used to enrich significant pathways.

Results

Physiological and biochemical index analysis

KKAy mice were used as model animals for the induction of type 2 diabetes by HFD. We successfully established a type 2 diabetes model and examined BW, FBG physiological indicators, and serum lipid biochemical indicators. The BW and FBG levels were substantially higher in the model group than in the control group (Fig. 2A and B); the serum TC, TG, and LDL-C contents were significantly higher, whereas the HDL-C content was considerably lower (Fig. 2C–F). After 7 days of treatment with ST, GTRH, GTRM, GTRL, and GTS, the serum FBG, TC, TG, HDL-C, and LDL-C levels of KKAy mice were improved to different degrees. Among them, the therapeutic effect of GTR was more significant than that of ST, with GTRH showing a greater effect than GTRM and GTRL. However, GTS showed no noticeable improvement.

Histopathological analysis of the kidney and pancreas

The histopathological changes in the kidney and pancreas in the control, model, Met, ST, GTRH, GTRM, GTRL, and GTS groups were examined under a light microscope after 7 days of administration. In the control group, the renal tissue structure, including the cortex and medulla, was intact and normal. In the model group, the renal tubules became basophilic and partially necrotic. (Fig. 3).

In the Met group, the renal tissue structure was complete, and no other pathological alterations were detected. In the ST group, the renal tubules were disarranged, with extensive degeneration and necrosis of renal tubular epithelial cells, and dilatation of the tubular lumens. In the GTRH group, the renal tissue structure was complete and normal. In the GTRM and GTRL groups, the renal tissue structure was complete, mild degeneration of a few renal tubular epithelial cells. However, the renal tissue structure in the GTS group was very similar to that in the model group. In the control group, the pancreatic tissue structure, including the pancreatic islets and

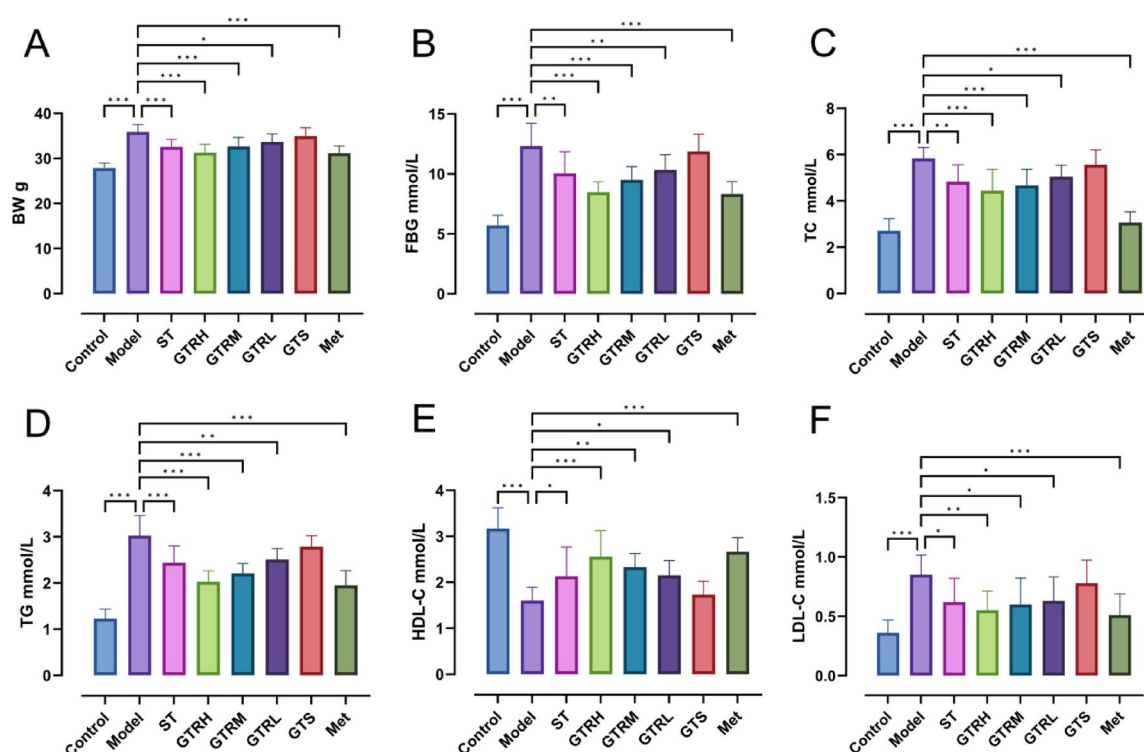


Fig. 2. Effects on serum lipids of mice after 7 days of drug administration. (A) Body weight; (B) Fasting blood glucose; (C) Total cholesterol; (D) Triacylglycerol; (E) High-density lipoprotein cholesterol; (F) Low-density lipoprotein cholesterol; * $P < 0.05$, ** $P < 0.01$, and *** $P < 0.001$ vs Model.

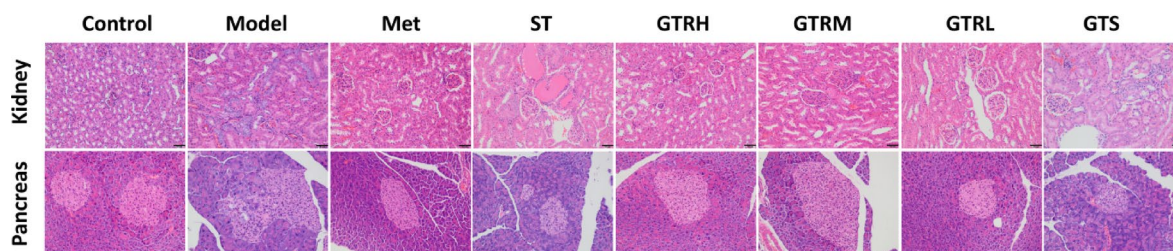


Fig. 3. Observation of histopathology of kidney and pancreas by HE staining under light microscope ($\times 200$). Scale bar represents 50 μm .

exocrine parts, was intact and normal. In the model group, the pancreatic islets showed atrophy with indistinct boundaries, extensive degeneration of islet β cells, and swelling of exocrine cells. In the Met group, the pancreatic tissue structure was complete and normal. In the ST group, the pancreatic islets showed atrophy with unclear boundaries, a reduction in the number of β cells, and occasional degeneration of β cells. In the GTRH group, the structure of the pancreas was complete and normal. In the GTRM group, the pancreatic tissue structure was complete and included mainly islets and exocrine parts. The number of β cells within the islets decreased slightly, and pancreatic cell degeneration were observed occasionally. In the GTRL group, the pancreatic tissue structure was complete, and the islet area decreased relative to that in the positive control group. The number of β cells in the islets decreased slightly, and slight degeneration of β cells was occasionally observed. In the GTS group, the islet volume was atrophic, the islet boundary was indistinct, the β cells were slightly denatured. The histopathological results revealed that the pathologic changes in kidney and pancreas tissues improved to different degrees in the different treatment groups; the changes were most prominent in the Met group, followed by the GTRH group. However, no prominent improvement was observed in the GTS group (Fig. 3). Because GTRH group showed better therapeutic effect than GTRM, and GTRL group in the physiological and biochemical experiments, only GTRH group was used in non-targeted metabolomics analysis.

Multivariate statistical analysis of serum metabolites

Serum samples from each group were ionized by ESI in both ion modes, and a representative chromatogram is shown in Fig. 4. After the raw data were input into the Progenesis QI software, 2478 positive ions and 789 negative ions were detected. We also input the normalized data in the SIMCA-P software to conduct multivariate regression. The OPLS-DA and PCA score plots revealed a significant separation between the model and control groups, with significantly different metabolic profiles between them (Figs. 5A and B and 6A and B). A permutation test of OPLS-DA was also conducted to verify whether this analytical model was feasible. The blue Q2 values on the left decreased relative to the original points on the right, and the blue regression line for the Q2 points intersected with the vertical axis below zero, which indicated that the analytical models were feasible (Figs. 5C and 6C). R2 and Q2 are also common parameters for evaluating analytical models in OPLS-DA. R2 and Q2 values closer to 1 indicate that the analytical model is closer to the real experimental model. In the positive ion mode, the cumulative R2X, R2Y, and Q2 values were 0.882, 0.988, and 0.913, respectively, whereas those in the negative ion mode were 0.767, 0.946, and 0.893, respectively. The results of the multivariate statistical analysis suggested the existence of differential metabolites between normal and KKAY mice.

Selection and identification of serum biomarkers

The S-plots and VIP-plots based on the OPLS-DA revealed changes in and correlations between the differential metabolites in serum, respectively (Figs. 5D and 6D). Based on the p -value of Student's t -test and OPLS-DA analyses, differential metabolites in serum satisfying $P < 0.05$ and $\text{VIP} > 1$ were considered biomarkers for preliminary screening. Then, the differential metabolites were compared with databases, such as HMDB (<https://hmdb.ca/>) and MassBank (<https://massbank.eu/MassBank/>), and those reported in published studies, via MS. Receiver operating characteristic (ROC) curves are commonly used to predict the disease diagnostic capacity of various biomarkers in the clinic. An ROC curve closer to the upper-left corner indicated more accurate biomarkers for predicting T2D (Fig. 7C). An area under the curve (AUC) close to 1 suggests a more accurate proof. Generally, biomarkers with AUC values greater than 0.65 suggest a strong ability to predict diseases. In this study, the AUCs exceeded 0.65, which indicated that the biomarkers can be used to predict T2D (Fig. 7A). In total, 15 potential biomarkers were characterized (Table 1). The information on the AUC and P -values for each potential serum biomarker is displayed in Table 2. The potential serum biomarkers included six amino acids (glycine, L-leucine, L-valine, etc.), four carbohydrates (citric acid, D-glucose, D-galactose, etc.), two fatty acids (oleic acid and linoleic acid), two glycerophospholipids (LysoPC(15:0), LysoPC(20:0)), and one nucleotide (uric acid). The changes in the content of potential serum biomarkers are shown in Fig. 7B. Among these 15 biomarkers, 11 were upregulated, and four were downregulated in the model group relative to their expression in the control group.

Regulation of biomarkers by ST, GTR, and GTS

The PCA score plots for the medication regulation of KKAY mice are shown in Fig. 8. The results showed that the six groups were preliminarily separated. There is a statistically significant difference between the model and control groups. When each treatment group is compared with the control group, the order of differences

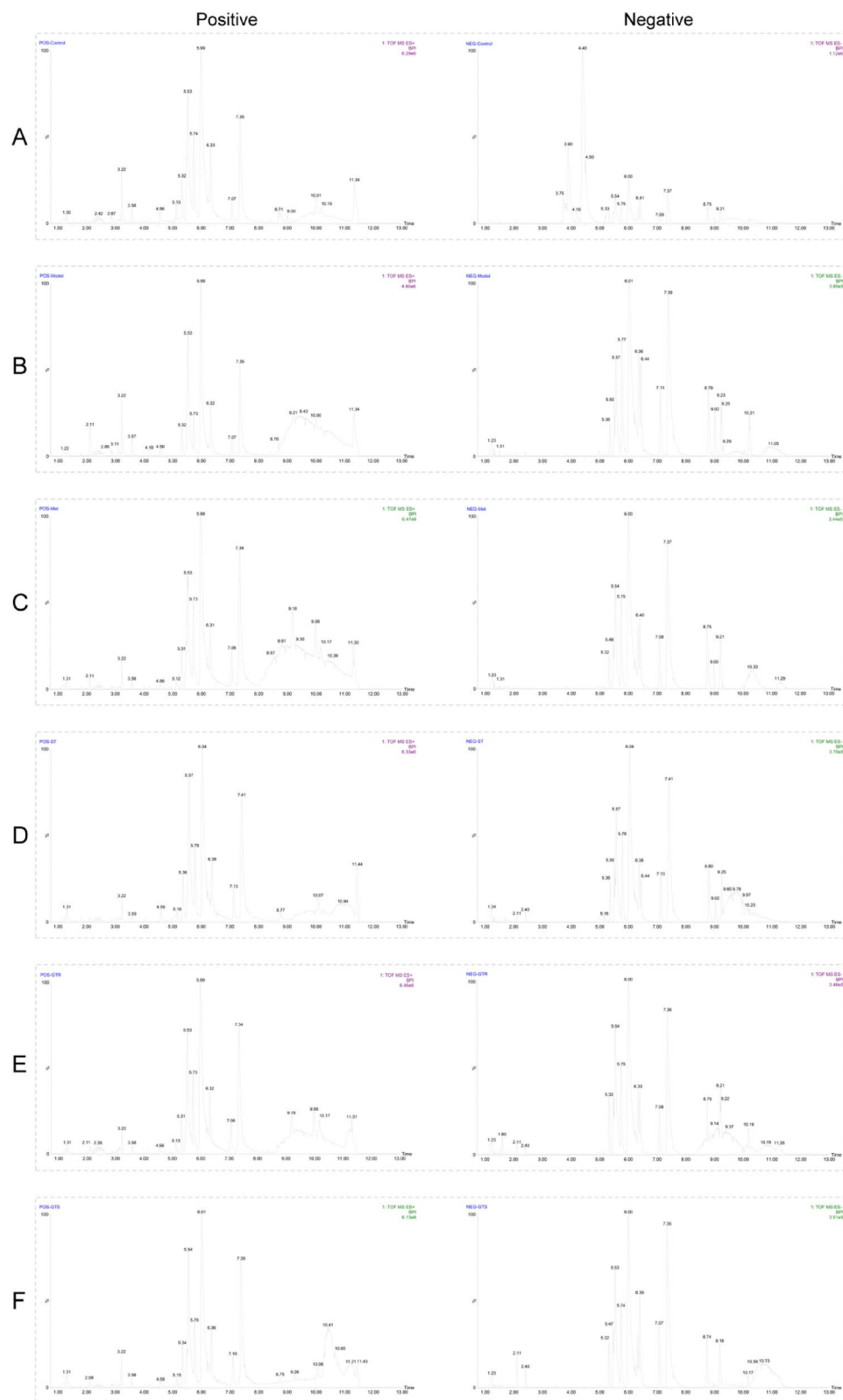


Fig. 4. The BPI chromatogram of serum samples in positive and negative ion modes by UPLC-Q/TOF-MS. (A) Control group. (B) Model group. (C) Met group. (D) ST group. (E) GTR group. (F) GTS group.

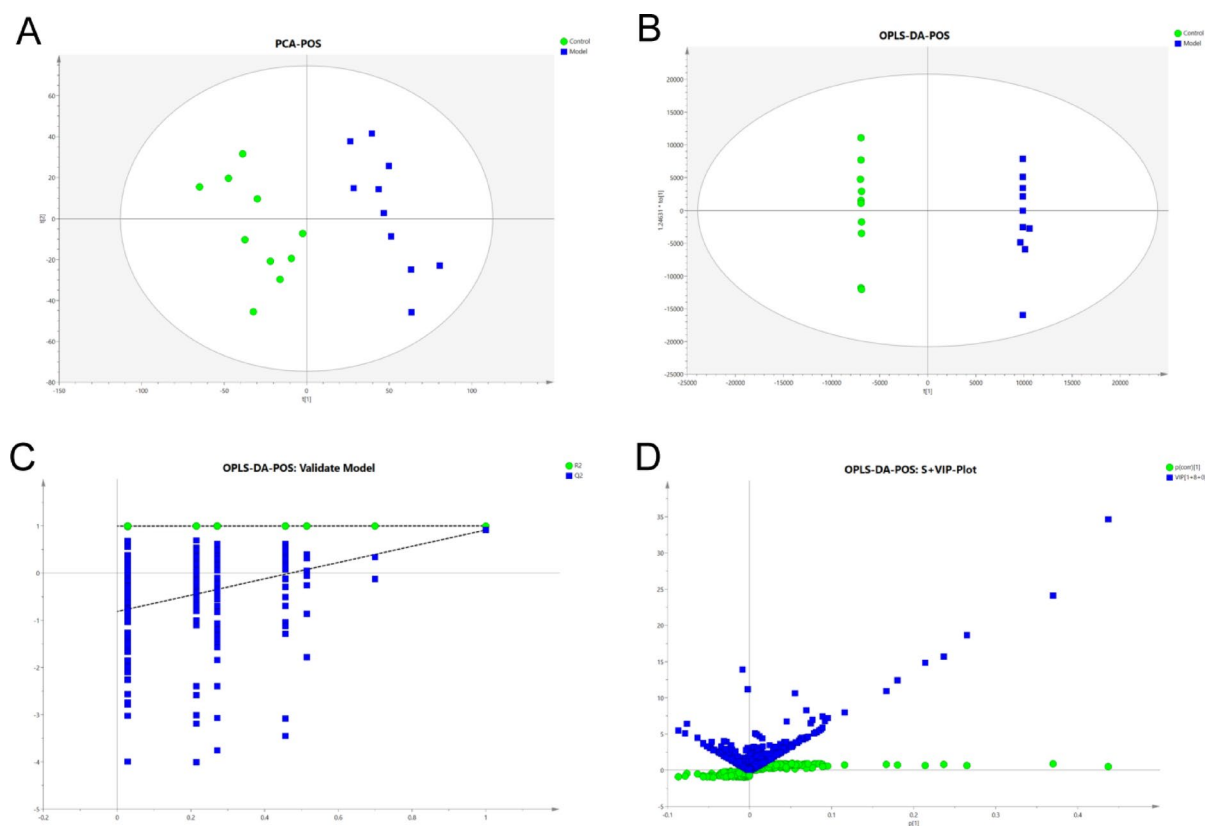


Fig. 5. Multivariate analysis of control group and model group in positive ion mode. **(A)** PCA scores plot. **(B)** OPLS-DA score plot. **(C)** OPLS-DA-Permutation test. **(D)** OPLS-DA-S+VIP score plots.

from small to large is as follows: Met group, GTR group, ST group, and GTS group. (Fig. 8A, B). These results indicated that GTR could regulate metabolic disorders in T2D more effectively than ST or GTS. Hierarchical clustering heatmap analysis of 10 serum biomarkers revealed differences in the relative contents among the six groups (Fig. 9), in which luminance fluctuations in color altered the levels of biomarkers. Eight biomarkers were downregulated, and two biomarkers were upregulated in the GTR group compared to their expression in the model group. These biomarkers included three amino acids (glycine, L-leucine, and L-valine), four carbohydrates (citric acid, D-glucose, D-galactose, and D-glutamine), one nucleotide (uric acid), and two glycerophospholipids (LPC (15:0) and LPC (20:0)). The biomarker levels recorded in the GTR and ST groups are shown in Fig. 10. The relative contents of the serum biomarkers changed significantly after treatment, and GTR altered the biomarkers more effectively than ST.

Metabolic pathway analysis

The results of the metabolic pathway analyses performed using the MetaboAnalyst 5.0 platform showed that the potential serum biomarkers were mostly related to glyoxylate and dicarboxylate metabolism; glycine, serine, and threonine metabolism; glutathione metabolism; the citrate cycle (TCA cycle); galactose metabolism; primary bile acid biosynthesis; purine metabolism; and glycerophospholipid metabolism (Fig. 11). The mechanism underlying GTR intervention in T2D is shown in Fig. 12. Glycine was found to be involved in glycine, serine, and threonine metabolism, which is the main pathway through which GTR regulates T2D.

Discussion

Swertia is a traditional Chinese medicinal herb commonly used to treat various diseases, and it has been used in the clinic for more than 1000 years. ST, the predominant ingredient of *Swertia*, has strong antidiabetic activity^{17–19}. However, the bioavailability of ST is very low, and it can be metabolized quickly to other metabolites. Although several nitrogen-containing metabolites were also observed besides GTR and GTS after oral administration of gentianine, only GTR and GTS were detected in the plasma after oral administration of ST^{16,20}. Previous studies focused on the efficacy of ST in protecting the liver and promoting bile flow¹³. However, the efficacy of GTR and GTS in the treatment of T2D remains unreported, specifically, their antidiabetic mechanism needs to be determined by metabolomics. Metabolomics is a technology that uses different metabolic profiles to diagnose, treat, and predict diseases, ultimately explaining their overall mechanism of action^{21–27}. The characteristics of comprehensive metabolomics analysis are consistent with the concept of holism in traditional Chinese medicine (TCM). Revealing the nature of the disease and the mechanism of action of TCM by metabolomics is important for developing more efficient treatment strategies^{28–30}.

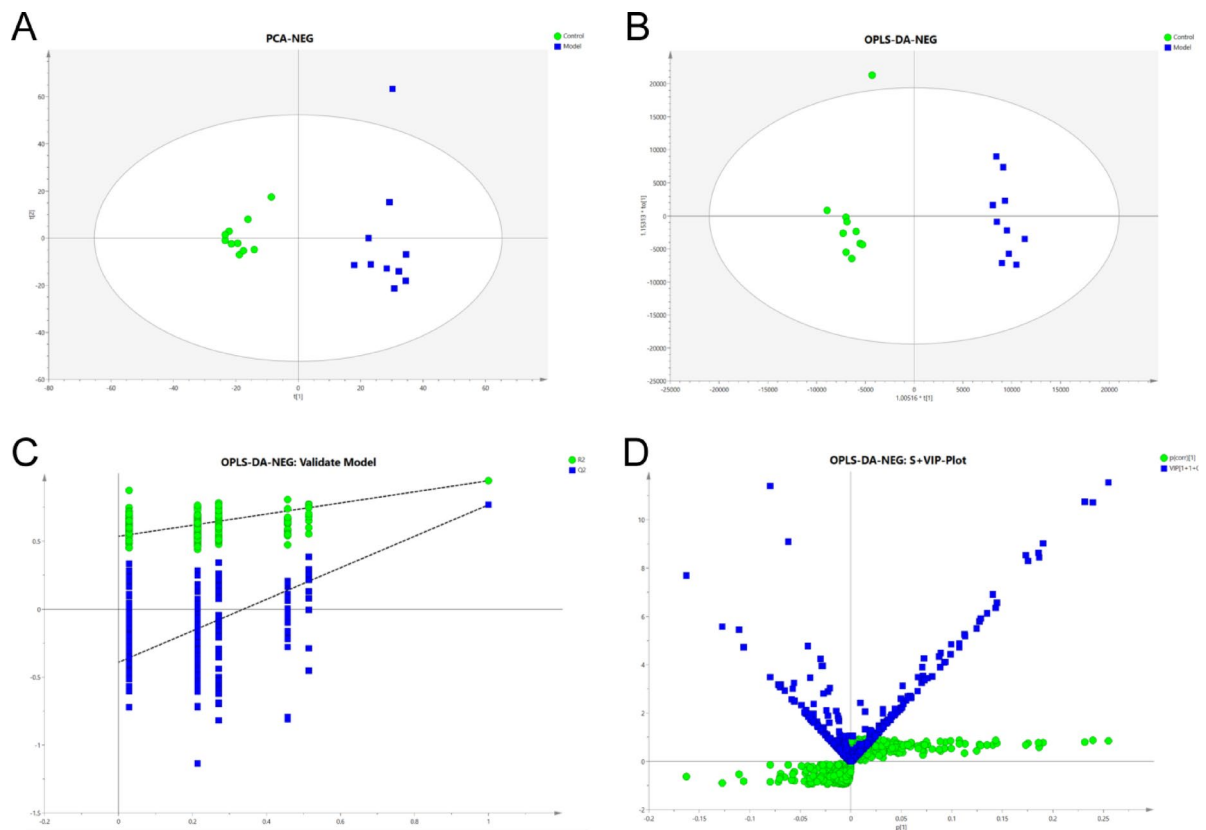


Fig. 6. Multivariate analysis of control group and model group in negative ion mode. (A) PCA scores plot. (B) OPLS-DA score plot. (C) OPLS-DA-Permutation test. (D) OPLS-DA-S+VIP score plots.

Metabolomic technology was used to identify biomarkers of KKAY mice to determine their dynamic temporal and spatial characteristics. Histopathology and lipid-related indicators were used to evaluate the roles of ST, GTR, and GTS in improving T2D. The metabolic pathways and mechanisms underlying the therapeutic effects of ST, GTR, and GTS on T2D were preliminarily explained by serum metabolomics. The levorotatory nitrogen-containing metabolite GTR showed stronger antidiabetic activity than the original compound ST; however, GTS showed no prominent antidiabetic activity. We found that 10 potential biomarkers significantly affected clustering and were altered by GTR. Eight main metabolic pathways associated with T2D were identified by tracking metabolic pathways associated with alterations in biomarkers. Glycine was found to be the most important biomarker for GTR to regulate T2D, and its involvement in glycine, serine, and threonine metabolism was also found to be a key regulatory pathway.

Glycine, serine, and threonine metabolism: Alanine-glyoxylate aminotransferase (AGT) is the pyridoxal 5'-phosphate (PLP)-dependent enzyme distributed in peroxisomes and catalyzes glyoxylate to form glycine³¹, thus exerting the detoxification effect of glyoxylic acid³². AGT participates in the metabolic pathways of glyoxylate and dicarboxylate metabolism; glycine, serine, and threonine metabolism; and gluconeogenesis³³. Congenital absence of AGT leads to primary type 1 hyperuricemia. In such patients, glyoxylate cannot be effectively degraded, and it is converted to calcium oxalate and deposited in renal calcium^{34,35}. The glycine level is negatively correlated with insulin resistance, and a decrease in glycine concentration may serve as an early marker of T2D³⁶. To summarize, the mistargeting of mitochondria by AGT can result in abnormal glyoxylate conversion to glycine, and a decrease in glycine concentration can lead to insulin resistance followed by T2D. As shown by the metabolic data, the serum glycine level in KKAY mice with T2D significantly decreased, causing abnormal glycine, serine, and threonine metabolism. The glycine level in KKAY mice with T2D increased significantly after treatment with GTR, which suggested that GTR exhibits an antidiabetic effect by regulating the glycine, serine, and threonine metabolic pathways.

TCA cycle: The TCA cycle occurs mainly in the mitochondria. Proteins, sugars, and lipids can be converted directly or indirectly by the TCA cycle³⁷. Acetyl-CoA can be produced by the β -oxidation of fatty acids and the oxidative decarboxylation of pyruvic acid after glycolysis. It is also known as activated acetic acid and participates in the TCA cycle³⁸. When patients with T2D lack insulin, lipolysis accelerates, and the production of acetyl-CoA increases, resulting in the accumulation of high concentrations of citric acid^{39,40}. The citric acid content in the serum of KKAY mice increased significantly. The content of citric acid returned to a level similar to that found in the control after treatment with GTR and ST, which suggested that the TCA cycle was promoted and normal metabolism of proteins, sugars, and lipids occurred.

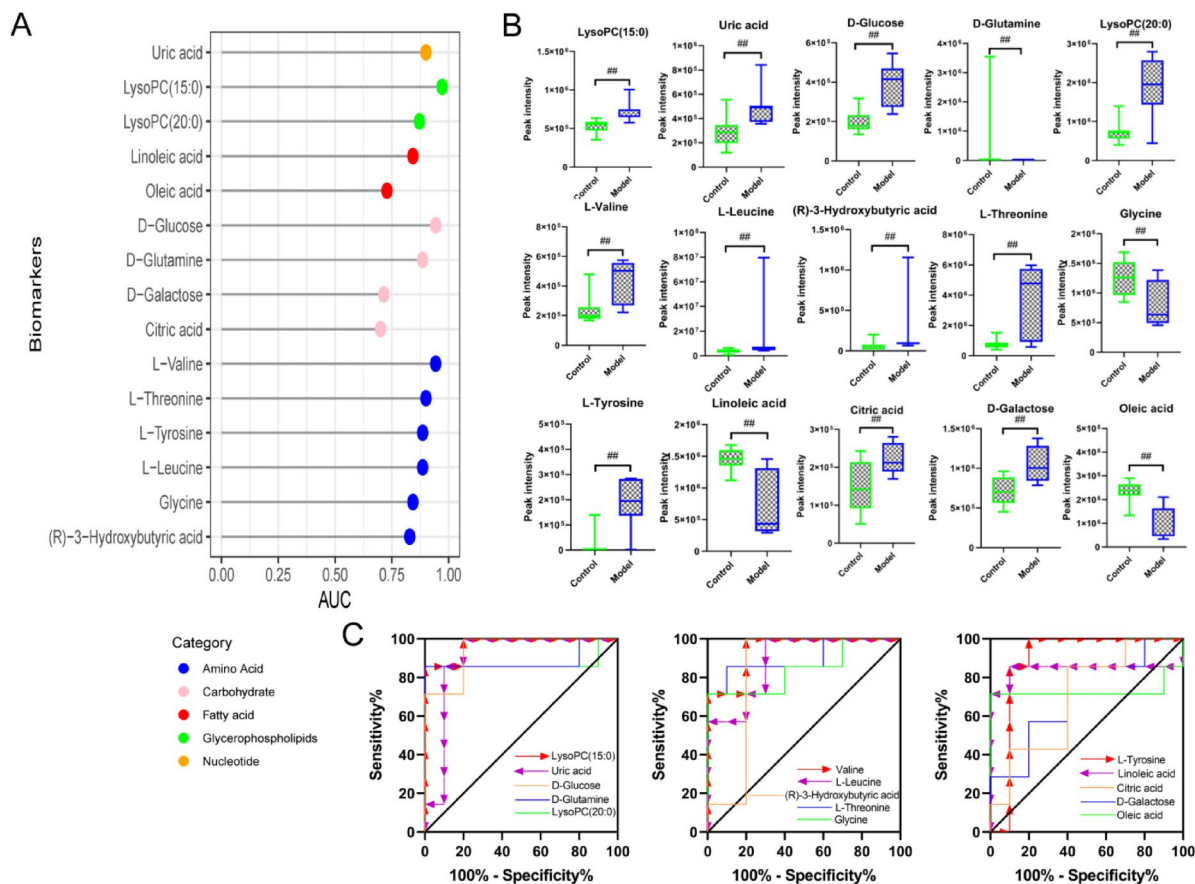


Fig. 7. Potential serum biomarkers with favorable diagnostic efficiency and biological significance in the control and model groups. **(A)** Cleveland dot map of 15 biomarkers. The dot per biomarker indicates the AUC in the control and model groups. Different colors represent different categories. **(B)** Box plots showing the relative strength of 15 biomarkers in the control and model groups. ## $P < 0.01$ vs control. **(C)** ROC curves of 15 potential serum biomarkers.

No.	RT/min	m/z	Adducts	Formula	Error/ppm	Compound	Mass fragments	M vs C
1	1.23	167.0158	M-H	$C_5H_4N_4O_3$	1.27	Uric acid	124.0212;69.0100;41.9978	↑
2	1.31	179.0556	M-H	$C_6H_{12}O_6$	0.93	D-Galactose	89.0248;59.0641	↑
3	5.36	179.1000	M-H	$C_6H_{12}O_6$	1.97	D-Glucose	89.1440;70.2332;59.0120	↑
4	2.11	147.0770	M+H	$C_5H_{10}N_2O_3$	1.93	D-Glutamine	101.0715;84.0449;56.0500	↓
5	5.57	180.0399	M-H	$C_9H_{11}NO_3$	2.03	L-Tyrosine	119.0350;72.0661	↑
6	3.22	118.0809	M+H	$C_5H_{11}NO_2$	2.39	L-Valine	72.0868	↑
7	5.32	132.0182	M+H	$C_6H_{13}NO_2$	-1.78	L-Leucine	111.1007	↑
8	5.77	279.0099	M-H	$C_{18}H_{32}O_2$	2.55	Linoleic acid	128.2334	↓
9	5.53	193.0290	M+H	$C_6H_8O_7$	-2.41	Citric acid	133.0031;115.0348;61.0137	↑
10	5.99	482.3237	M-H	$C_{23}H_{48}NO_7P$	4.92	LysoPC(15:0)	184.0728;104.1067	↑
11	6.32	552.3918	M+H	$C_{28}H_{58}NO_7P$	3.33	LysoPC(20:0)	534.0733;184.1070;104.4024	↑
12	6.01	281.3122	M-H	$C_{18}H_{34}O_2$	1.40	Oleic acid	263.2488	↓
13	7.35	105.0441	M+H	$C_4H_8O_3$	-1.92	(R)-3-Hydroxybutyric acid	87.0335;69.0546	↑
14	10.00	120.0555	M+H	$C_4H_9NO_3$	4.37	L-Threonine	102.0290;56.0606	↑
15	11.34	76.0293	M+H	$C_2H_5NO_2$	1.98	Glycine	58.0344;30.0399	↓

Table 1. Annotation of potential serum biomarkers in KKAY mice.

Biomarkers	AUC (95% CI)	P-value
LysoPC (15:0)	0.9714 (0.9006–1.000)	< 0.01
Uric acid	0.9000 (0.7329–1.000)	< 0.01
D-Glucose	0.9429 (0.8366–1.000)	< 0.01
D-Glutamine	0.8857 (0.6728–1.000)	< 0.01
LysoPC (20:0)	0.8714 (0.6353–1.000)	< 0.01
L-Valine	0.9429 (0.8366–1.000)	< 0.01
L-Leucine	0.8857 (0.7273–1.000)	< 0.01
(R)-3-Hydroxybutyric acid	0.8286 (0.6074–1.000)	< 0.01
L-Threonine	0.9000 (0.7301–1.000)	< 0.01
Glycine	0.8429 (0.6294–1.000)	< 0.01
L-Tyrosine	0.8857 (0.6974–1.000)	< 0.01
Linoleic acid	0.8429 (0.5841–1.000)	< 0.01
Citric acid	0.7000 (0.4436–0.956)	< 0.01
D-Galactose	0.7143 (0.4578–0.971)	< 0.01
Oleic acid	0.7286 (0.4080–1.000)	< 0.01

Table 2. Diagnostic efficiency of 15 biomarkers in the control and model groups.

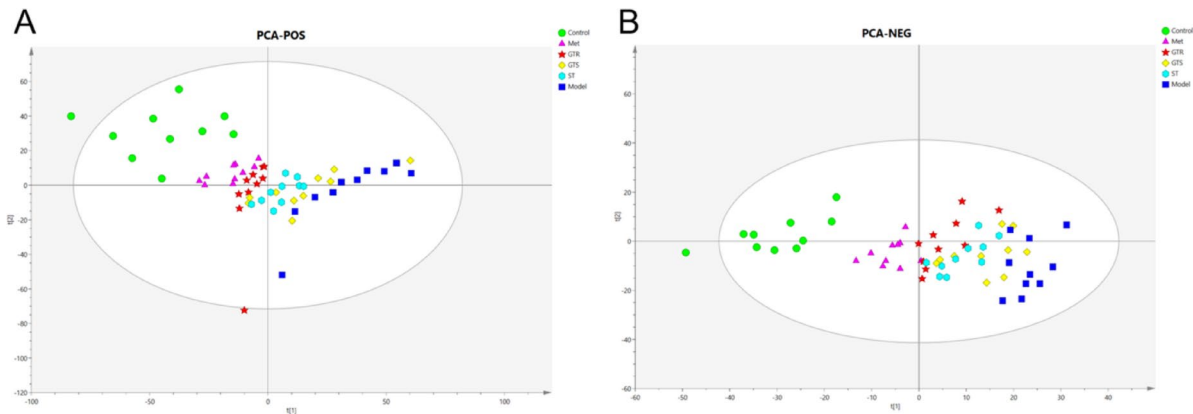


Fig. 8. The PCA score plots of the serum metabolites in different groups with treatment. (A) In positive ion mode. (B) In negative ion mode.

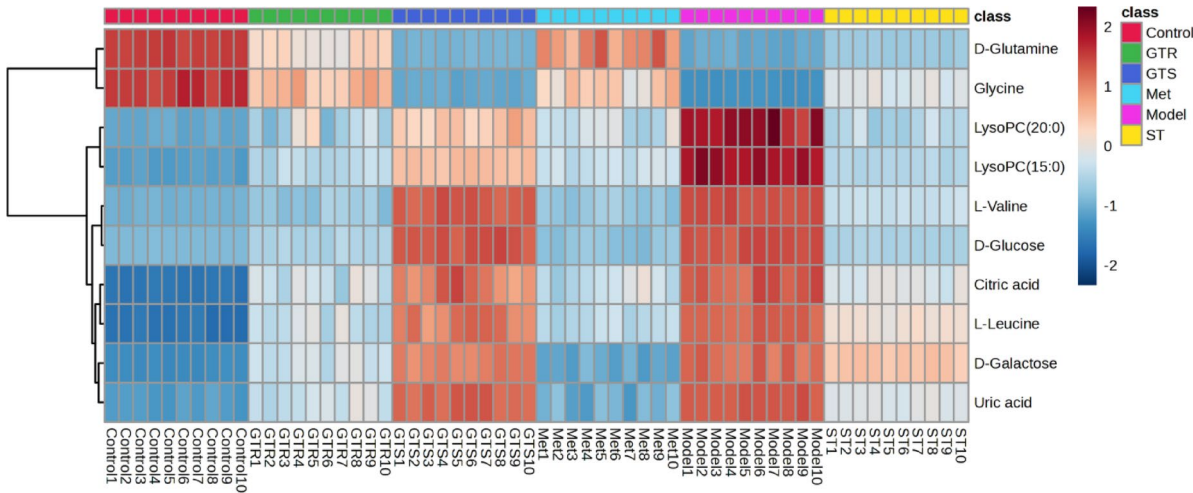


Fig. 9. Hierarchical clustering heatmap of potential serum biomarkers after treatment among six groups. The degree of change is marked with colors, with red indicating up-regulation and blue indicating down-regulation.

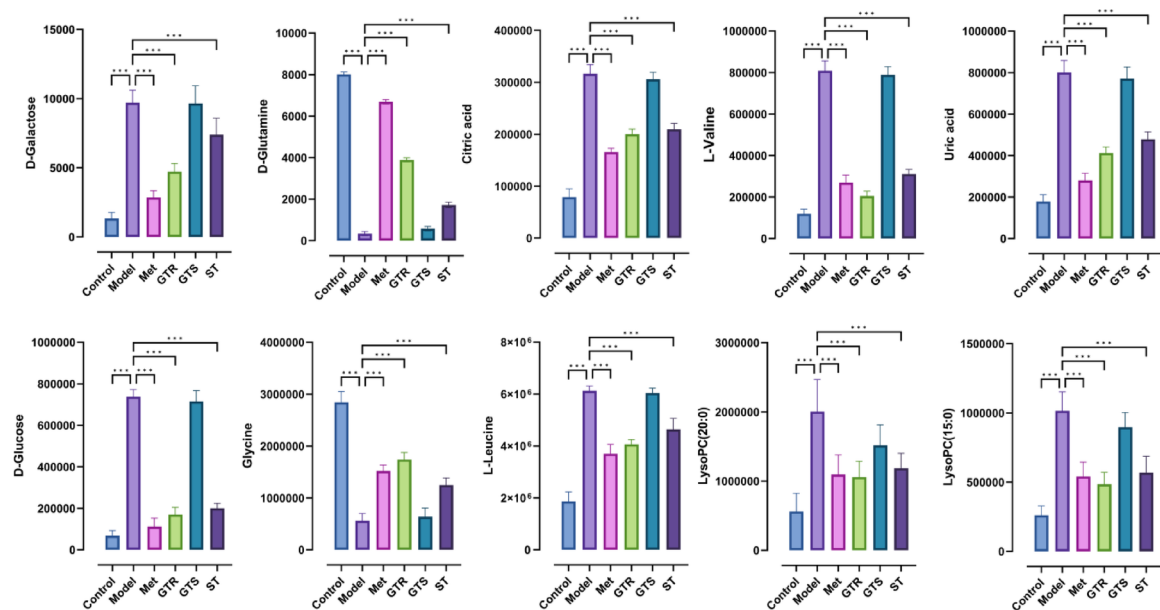


Fig. 10. Comparison of relative strength of potential serum biomarkers among different groups after treatment, in which the level of glycine and L-leucine observably changed after treatment compared with the model group. * $P < 0.05$, ** $P < 0.01$, and *** $P < 0.001$ vs Model.

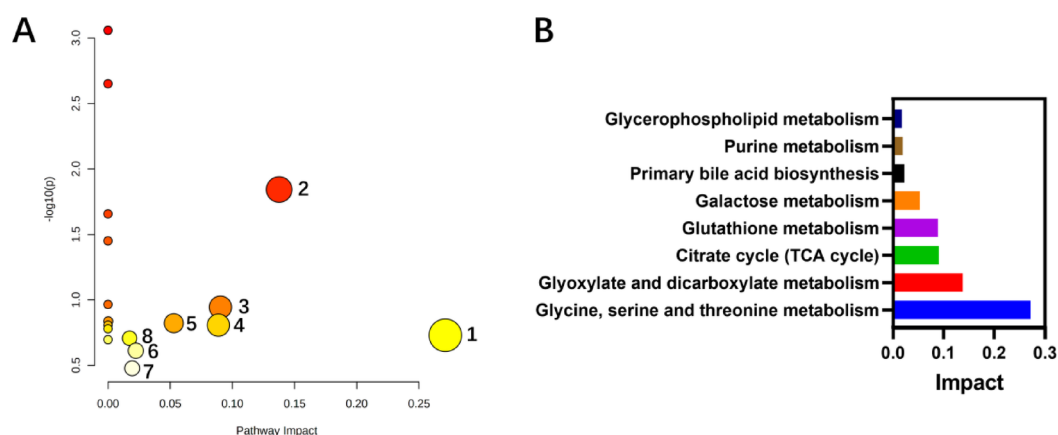


Fig. 11. Enrichment analysis of potential serum biomarkers metabolic pathways in KKAY type 2 diabetic mice after treatment of GTR. (A) Overview diagram of pathway analysis by MetPA 5.0. (B) Histogram of main metabolic pathways impact. (1) Glycine, serine, and threonine metabolism; (2) Glyoxylate and dicarboxylate metabolism; (3) Citrate cycle (TCA cycle); (4) Glutathione metabolism; (5) Galactose metabolism; (6) Primary bile acid biosynthesis; (7) Purine metabolism; (8) Glycerophospholipid metabolism.

Galactose metabolism: Galactose metabolism is the intersection of glycolysis and glycosylation. It is usually characterized by the metabolism of galactose and uridine diphosphate-glucose (UDP-Glu) to uridine diphosphate-galactose (UDP-Gal) through galactose mutarotase (GALM), galactose-1-phosphate uridylyltransferase (GALT), and galactokinase (GALK). Abnormal UDP-Gal upregulation leads to aberrant glycosylation, which produces advanced glycation end products, further leading to T2D⁴¹. The galactose content in KKAY mice increased, indicating that T2D caused abnormal galactose metabolism. GTR and ST effectively corrected the abnormal increase in galactose levels and regulated the balance of galactose metabolism.

Purine metabolism: The content of uric acid in KKAY mice increased, indicating that purine metabolism is related to T2D. Almost all purine compounds can be oxidized to uric acid in vivo^{42,43}. Uric acid serves as a potent free radical scavenger in humans; however, hyperuricemia probably leads to β -cell dysfunction or insulin resistance⁴⁴. Purine metabolic disorders can accelerate xanthine oxidoreductase (XOR) production, thus increasing uric acid levels, resulting in hyperuricemia^{43,45} and β -cell dysfunction in T2D⁴⁶, accompanied by T2D nephropathy⁴⁷. ST and GTR regulate purine metabolism to return uric acid levels to normal.

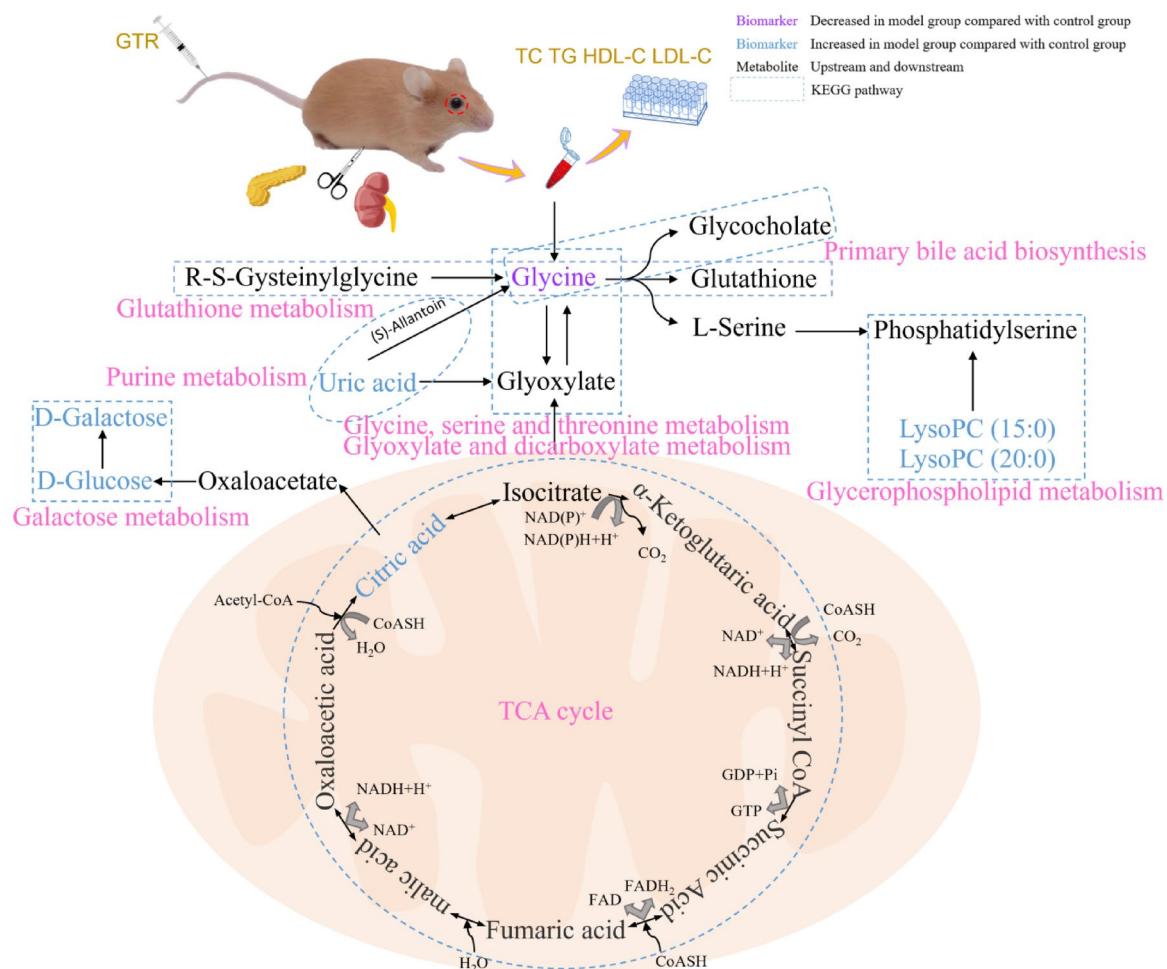


Fig. 12. Mechanism of GTR intervention in T2D. Purple font: biomarkers that decreased in the model group and were recalled by GTR. Blue font: biomarkers that increased in the model group and were recalled by GTR. Blank font: upstream and downstream metabolites. Dashed box: KEGG pathways. (The mice IMAGE in this figure is adapted from: <http://www.hfkbio.com/cms/item/view?table-product&id=42#> with permission from Beijing HFK Bioscience Co., Ltd. Figure was generated by PowerPoint 2021: <https://www.microsoft.com/zh-cn/microsoft-365/powerpoint#Mobile-download>).

Glycerophospholipid metabolism: T2D is often accompanied by hyperlipidemia and hypertension^{48–50}. T2D may further progress after kidney injury and possibly lead to hypertension^{51,52}. Moreover, hyperlipidemia is also a risk factor for T2D⁵³. Glycerophospholipid may influence insulin sensitivity in T2D patients, confirming the relationship between glycerophospholipid metabolism and T2D⁵⁴. As glycerophospholipids are highly abundant in mammals, an increase in the content of LysoPCs inhibits sarcoendoplasmic reticulum Ca^{2+} -ATPase (SERCA), causing endoplasmic reticulum (ER) stress and eventually stimulating insulin resistance^{55,56}. In this study, we found that the serum LysoPC(15:0) and LysoPC(20:0) levels in model mice were higher. This increase occurred probably because of diacylglycerol (DG) expression, which led to an increase in serum lipids. GTR effectively decreased the content of LysoPCs by regulating glycerophospholipid metabolism.

Other metabolic pathways: Glycine is produced by glyoxylate under the catalysis of glutamate-glyoxylate aminotransferase, which in turn regulates glyoxylate and dicarboxylate metabolism. Glycine is converted into glutathione through glutathione synthetase, thus affecting glutathione metabolism. Under the action of bile acid-CoA, primary bile acid biosynthesis is influenced by the conversion of glycine to glycocholate. Studies have shown that an increase in valine and leucine levels and a decrease in glutamine levels are significantly associated with T2D^{57–60}.

Conclusion

The non-targeted serum metabolism method was used for the first time in this study to identify representative biomarkers associated with the antidiabetic efficacy of GTR, and the associated metabolic pathways were analyzed and explained. Additionally, blood glucose, biochemical indicators of lipids, and histopathological tests were used as auxiliary tools to investigate the pharmacological mechanism underlying the therapeutic effects

of ST, GTR, and GTS on KKAY type 2 diabetic mice. Among them, treatment with GTR showed significant improvement in KKAY type 2 diabetic mice. We identified 15 endogenous biomarkers, 10 of which were recalled by GTR, and glycine was the most effectively recalled by GTR and regulated eight metabolic pathways. Specifically, the metabolism of glycine, serine, and threonine was significantly affected. The mechanism for GTR to regulate T2D was elucidated and GTR exhibited great potential as an effective drug to improve T2D.

Data availability

The data that support the findings of this study are available from the corresponding author upon reasonable request.

Received: 15 November 2024; Accepted: 28 April 2025

Published online: 06 May 2025

References

- Ghasemi, A. & Norouzirad, R. Type 2 diabetes: An updated overview. *Crit. Reviews™ Oncog.* **24**, 213–222. <https://doi.org/10.1615/critrevoncog.2019030976> (2019).
- Magliano, D. J. & Boyko, E. J. IDF Diabetes Atlas, 10th edition (2021).
- World Health Organization. *The top 10 causes of death, Available from: The top 10 causes of death* (2020).
- Chung, I. M. et al. Insights on the current status and advancement of diabetes mellitus type 2 and to avert complications: An overview. *Biotechnol. Appl. Chem.* **67**, 920–928. <https://doi.org/10.1002/bab.1853> (2020).
- Ortiz-Martínez, M. et al. Recent developments in biomarkers for diagnosis and screening of type 2 diabetes mellitus. *Curr. Diab. Rep.* **22**, 95–115. <https://doi.org/10.1007/s11892-022-01453-4> (2022).
- Rosengren, A. Cardiovascular disease in diabetes type 2: Current concepts. *J. Intern. Med.* **284**, 240–253. <https://doi.org/10.1111/j.oim.12804> (2018).
- Xiong, X. et al. Family history of diabetes is associated with diabetic foot complications in type 2 diabetes. *Sci. Rep.* **10**, 17056. <https://doi.org/10.1038/s41598-020-74071-3> (2020).
- Thipsawat, S. Early detection of diabetic nephropathy in patient with type 2 diabetes mellitus: A review of the literature. *Diabetes Vasc. Dis. Res.* **18**, 14791641211058856. <https://doi.org/10.1177/14791641211058856> (2021).
- Slomski, A. New data on retinopathy in youth-onset type 2 diabetes. *JAMA* **327**, 416. <https://doi.org/10.1001/jama.2022.0149> (2022).
- Gallart-Ayala, H., Teav, T. & Ivanisevic, J. Metabolomics meets lipidomics: Assessing the small molecule component of metabolism. *BioEssays* **42**, 2000052. <https://doi.org/10.1002/bies.202000052> (2020).
- Trifonova, O. P., Maslov, D. L., Balashova, E. E. & Lokhov, P. G. Mass spectrometry-based metabolomics diagnostics—myth or reality? *Expert Rev. Proteom.* **18**, 7–12. <https://doi.org/10.1080/14789450.2021.1893695> (2021).
- Ma, Q. et al. Progress in metabolomics of type 2 diabetes mellitus. *Molecules* **23**, 1834. <https://doi.org/10.3390/molecules23071834> (2018).
- Shi, M., Tang, J., Zhang, T. & Han, H. Swertiamarin, an active iridoid glycoside from *Swertia pseudochinensis* H. Hara, protects against alpha-naphthylisothiocyanate-induced cholestasis by activating the farnesoid X receptor and bile acid excretion pathway. *J. Ethnopharmacol.* **291**, 115164. <https://doi.org/10.1016/j.jep.2022.115164> (2022).
- Kumar, S. et al. Synthesis, molecular docking and ADMET prediction of novel Swertiamarin analogues for the restoration of type-2 diabetes: An enzyme inhibition assay. *Nat. Prod. Res.* **36**, 2197–2207. <https://doi.org/10.1080/14786419.2020.1825428> (2020).
- Vaidya, H., Goyal, R. K. & Cheema, S. K. Anti-diabetic activity of Swertiamarin is due to an active metabolite, gentianine, that upregulates PPAR-γ gene expression in 3T3-L1 cells. *Phytother. Res.* **27**, 624–627. <https://doi.org/10.1002/ptr.4763> (2013).
- Wang, Z., Wang, X., Sun, H., Chen, L. & Ma, C. Determination of novel nitrogen-containing metabolite after oral administration of Swertiamarin to rats. *J. Asian Nat. Prod. Res.* **14**, 176–181. <https://doi.org/10.1080/10286020.2011.631132> (2012).
- Sonawane, R. D. et al. Role of 5-HT₂ receptors in diabetes: Swertiamarin seco-iridoid glycoside might be a possible 5-HT₂ receptor modulator. *Physiol. Behav.* **144**, 66–72. <https://doi.org/10.1016/j.physbeh.2015.02.036> (2015).
- Li, J., Zhao, Y., Huang, H. & Wang, Y. Phytochemistry and Pharmacological activities of the genus *Swertia* (Gentianaceae): A review. *Am. J. Chin. Med.* **45**, 667–736. <https://doi.org/10.1142/s0192415x17500380> (2017).
- Patel, N., Tyagi, R. K., Tandel, N., Garg, N. K. & Soni, N. The molecular targets of Swertiamarin and its derivatives confer anti-diabetic and anti-hyperlipidemic effects. *Curr. Drug Targets* **19**, 1958–1967. <https://doi.org/10.2174/1389450119666180406113428> (2018).
- Li, H. L. et al. Determination of the plasma Pharmacokinetic and tissue distributions of Swertiamarin in rats by liquid chromatography with tandem mass spectrometry. *Arzneimittelforschung* **62**, 138–144. <https://doi.org/10.1055/s-0031-1298021> (2012).
- Moreau, R. et al. Blood metabolomics uncovers inflammation-associated mitochondrial dysfunction as a potential mechanism underlying ACLF. *J. Hepatol.* **72**, 688–701. <https://doi.org/10.1016/j.jhep.2019.11.009> (2020).
- Alseekh, S. et al. Mass spectrometry-based metabolomics: A guide for annotation, quantification and best reporting practices. *Nat. Methods* **18**, 747–756. <https://doi.org/10.1038/s41592-021-01197-1> (2021).
- Danlos, F. X. et al. Metabolomic analyses of COVID-19 patients unravel stage-dependent and prognostic biomarkers. *Cell Death Dis.* **12**, 258. <https://doi.org/10.1038/s41419-021-03540-y> (2021).
- Naylor, M., Brown, K. J. & Vasan, R. S. The molecular basis of predicting atherosclerotic cardiovascular disease risk. *Circul. Res.* **128**, 287–303. <https://doi.org/10.1161/circresaha.120.315890> (2021).
- Olsson, M., Hellman, U., Wixner, J. & Anan, I. Metabolomics analysis for diagnosis and biomarker discovery of transthyretin amyloidosis. *Amyloid* **28**, 234–242. <https://doi.org/10.1080/13506129.2021.1958775> (2021).
- Rispoli, M. G. et al. Contribution of metabolomics to multiple sclerosis diagnosis, prognosis and treatment. *Int. J. Mol. Sci.* **22**, 11112. <https://doi.org/10.3390/ijms22011112> (2021).
- Shi, Z., Zou, S., Shen, Z., Luan, F. & Yan, J. High-throughput metabolomics using UPLC/Q-TOF-MS coupled with multivariate data analysis reveals the effect and mechanism of syringin against ovariectomized osteoporosis. *J. Chromatogr. B.* **1183**, 122957. <https://doi.org/10.1016/j.jchromb.2021.122957> (2021).
- Han, Y., Sun, H., Zhang, A., Yan, G. & Wang X.-J. Chinmedomics, a new strategy for evaluating the therapeutic efficacy of herbal medicines. *Pharmacol. Ther.* **216**, 107680. <https://doi.org/10.1016/j.pharmthera.2020.107680> (2020).
- Zhang, Y. et al. Emerging applications of metabolomics to assess the efficacy of traditional Chinese medicines for treating type 2 diabetes mellitus. *Front. Pharmacol.* **12**, 735410. <https://doi.org/10.3389/fphar.2021.735410> (2021).
- Kong, L. et al. Chinmedomics strategy for elucidating the pharmacological effects and discovering bioactive compounds from Keluoxin against diabetic retinopathy. *Front. Pharmacol.* **13**, 728256. <https://doi.org/10.3389/fphar.2022.728256> (2022).
- Adeva-Andany, M. et al. Insulin resistance and glycine metabolism in humans. *Amino Acids* **50**, 11–27. <https://doi.org/10.1007/s00726-017-2508-0> (2018).

32. Ichiyama, A. Studies on a unique organelle localization of a liver enzyme, serine: Pyruvate (or alanine: glyoxylate) aminotransferase. *Proc. Jpn. Acad. Ser. B* **87**, 274–286. <https://doi.org/10.2183/pjab.87.274> (2011).
33. Miyajima, H., Oda, T. & Ichiyama, A. Induction of mitochondrial serine: Pyruvate aminotransferase of rat liver by glucagon and insulin through different mechanisms. *J. Biochem.* **105**, 500–504. <https://doi.org/10.1093/oxfordjournals.jbchem.a122695> (1989).
34. Cellini, B., Bertoldi, M., Montioli, R. & Paiardini, A. Borri Voltattorni, C. Human wild-type alanine: Glyoxylate aminotransferase and its naturally occurring G82E variant: Functional properties and physiological implications. *Biochem. J.* **408**, 39–50. <https://doi.org/10.1042/bj20070637> (2007).
35. Oppici, E. et al. Pyridoxamine and pyridoxal are more effective than pyridoxine in rescuing folding-defective variants of human alanine: Glyoxylate aminotransferase causing primary hyperoxaluria type I. *Hum. Mol. Genet.* **24**, 5500–5511. <https://doi.org/10.1093/hmg/ddv276> (2015).
36. Chen, L. et al. Glycine transporter-1 and glycine receptor mediate the antioxidant effect of glycine in diabetic rat Islets and INS-1 cells. *Free Radic. Biol. Med.* **123**, 53–61. <https://doi.org/10.1016/j.freeradbiomed.2018.05.007> (2018).
37. Choi, I., Son, H. & Baek, J. H. Tricarboxylic acid (TCA) cycle intermediates: Regulators of immune responses. *Life* **11**, 69. <https://doi.org/10.3390/life11010069> (2021).
38. Singh, P. K. et al. Metabolic profiling by gas chromatography-mass spectrometry of energy metabolism in high-fat diet-fed obese mice. *Plos One* **12** <https://doi.org/10.1371/journal.pone.0177953> (2017).
39. Mathew, A. V. et al. Impaired amino acid and TCA metabolism and cardiovascular autonomic neuropathy progression in type 1 diabetes. *Diabetes* **68**, 2035–2044. <https://doi.org/10.2337/db19-0145> (2019).
40. Villaseñor, A. et al. Metabolomics reveals citric acid secretion in mechanically-stimulated osteocytes is inhibited by high glucose. *Sci. Rep.* **9**, 2295. <https://doi.org/10.1038/s41598-018-38154-6> (2019).
41. Conte, F., van Buuringen, N., Voermans, N. C. & Lefeber, D. J. Galactose in human metabolism, glycosylation and congenital metabolic diseases: Time for a closer look. *Biochim. Et Biophys. Acta (BBA)-General Subj.* **1865**, 129898. <https://doi.org/10.1016/j.bbagen.2021.129898> (2021).
42. Huang, C. et al. Associations between serum uric acid and hepatobiliary-pancreatic cancer: A cohort study. *World J. Gastroenterol.* **26**, 7061–7075. <https://doi.org/10.3748/wjg.v26.i44.7061> (2020).
43. Liu, N. et al. The role of oxidative stress in hyperuricemia and Xanthine oxidoreductase (XOR) inhibitors. *Oxidative Med. Cell. Longev.* **2021** (1470380). <https://doi.org/10.1155/2021/1470380> (2021).
44. Binh, T. Q. et al. First report on association of hyperuricemia with type 2 diabetes in a Vietnamese population. *Int. J. Endocrinol.* **5275071**. <https://doi.org/10.1155/2019/5275071> (2019).
45. Furuhashi, M. New insights into purine metabolism in metabolic diseases: Role of Xanthine oxidoreductase activity. *Am. J. Physiol.-Endocrinol. Metab.* **319**, E827–E834. <https://doi.org/10.1152/ajpendo.00378.2020> (2020).
46. Li, G. X., Jiao, X. H. & Cheng, X. B. Correlations between blood uric acid and the incidence and progression of type 2 diabetes nephropathy. *Eur. Rev. Med. Pharmacol. Sci.* **22**, 506–511. https://doi.org/10.26355/eurrev_201801_14202 (2018).
47. Li, M., Gu, L., Yang, J. & Lou, Q. Serum uric acid to creatinine ratio correlates with β -cell function in type 2 diabetes. *Diab./Metab. Res. Rev.* **34** <https://doi.org/10.1002/dmrr.3001> (2018).
48. Liu, F. et al. Alterations of urinary microbiota in type 2 diabetes mellitus with hypertension and/or hyperlipidemia. *Front. Physiol.* **8**, 126. <https://doi.org/10.3389/fphys.2017.00126> (2017).
49. Ellulu, M. S., Naser, I. A., Abuhajar, S. M. & Najim, A. A. Determination of risk factors associated with inflammation in hypertensive patients with type-2 diabetes mellitus in a Palestinian diabetes study. *Curr. Med. Res. Opin.* **37**, 1451–1459. <https://doi.org/10.1080/03007995.2021.1941826> (2021).
50. Yuan, G. et al. Use of network pharmacology to explore the mechanism of Gegen (Puerariae lobatae Radix) in the treatment of type 2 diabetes mellitus associated with hyperlipidemia. *Evid. -Based Complement. Altern. Med.* **6633402**. <https://doi.org/10.1155/2021/6633402> (2021).
51. Lastra, G., Syed, S., Kurukulasuriya, L. R., Manrique, C. & Sowers, J. R. Type 2 diabetes mellitus and hypertension: An update. *Endocrinol. Metabolism Clin.* **43**, 103–122. <https://doi.org/10.1016/j.ecl.2013.09.005> (2014).
52. Horr, S. & Nissen, S. Managing hypertension in type 2 diabetes mellitus. *Best Pract. Res. Clin. Endocrinol. Metab.* **30**, 445–454. <https://doi.org/10.1016/j.beem.2016.06.001> (2016).
53. Matsuzaka, T. & Shimano, H. New perspective on type 2 diabetes, dyslipidemia and non-alcoholic fatty liver disease. *J. Diabetes Invest.* **11**, 532–534. <https://doi.org/10.1111/jdi.13258> (2020).
54. Fall, T. et al. Non-targeted metabolomics combined with genetic analyses identifies bile acid synthesis and phospholipid metabolism as being associated with incident type 2 diabetes. *Diabetologia* **59**, 2114–2124. <https://doi.org/10.1007/s00125-016-4041-1> (2016).
55. Albegali, A. A., Shahzad, M., Ullah, M. I., Mahmood, S. & Rashid, M. Association of genetic polymorphism of PC-1 gene (rs1044498 Lys121Gln) with insulin-resistant type 2 diabetes mellitus in Punjabi population of Pakistan. *Mol. Genet. Genom. Med.* **7** <https://doi.org/10.1002/mgg3.775> (2019).
56. Shetty, S. S. & Kumari, S. Fatty acids and their role in type-2 diabetes. *Exp. Ther. Med.* **22**, 706. <https://doi.org/10.3892/etm.2021.10138> (2021).
57. Vanweert, F. et al. Elevated plasma branched-chain amino acid levels correlate with type 2 diabetes-related metabolic disturbances. *J. Clin. Endocrinol. Metab.* **106**, e1827–e1836. <https://doi.org/10.1210/clinem/dgaa751> (2021).
58. Libert, D. M., Nowacki, A. S. & Natowicz, M. R. Metabolomic analysis of obesity, metabolic syndrome, and type 2 diabetes: Amino acid and acylcarnitine levels change along a spectrum of metabolic wellness. *PeerJ* **6** <https://doi.org/10.7717/peerj.5410> (2018).
59. Ren, W. et al. Glutamine metabolism in macrophages: A novel target for obesity/type 2 diabetes. *Adv. Nutr.* **10**, 321–330. <https://doi.org/10.1093/advances/nmy084> (2019).
60. White, P. J. et al. Insulin action, type 2 diabetes, and branched-chain amino acids: A two-way street. *Mol. Metab.* **52**, 101261. <https://doi.org/10.1016/j.molmet.2021.101261> (2021).

Acknowledgements

The authors thank everyone who contributed to the writing and all the publications and their authors involved in this study.

Author contributions

Y.X. and J.H. carried out the experimental part and wrote the first draft. S.T. provided the methodology. Y.S., H.L., and P.L. prepared figures and tables. X.L., M.H., X.W., and H.Z. revised the manuscript. Z.W. supervised the whole work and prepared the final manuscript. All authors reviewed the manuscript.

Declarations

Competing interests

The authors declare no competing interests.

Additional information

Correspondence and requests for materials should be addressed to Z.W.

Reprints and permissions information is available at www.nature.com/reprints.

Publisher's note Springer Nature remains neutral with regard to jurisdictional claims in published maps and institutional affiliations.

Open Access This article is licensed under a Creative Commons Attribution-NonCommercial-NoDerivatives 4.0 International License, which permits any non-commercial use, sharing, distribution and reproduction in any medium or format, as long as you give appropriate credit to the original author(s) and the source, provide a link to the Creative Commons licence, and indicate if you modified the licensed material. You do not have permission under this licence to share adapted material derived from this article or parts of it. The images or other third party material in this article are included in the article's Creative Commons licence, unless indicated otherwise in a credit line to the material. If material is not included in the article's Creative Commons licence and your intended use is not permitted by statutory regulation or exceeds the permitted use, you will need to obtain permission directly from the copyright holder. To view a copy of this licence, visit <http://creativecommons.org/licenses/by-nc-nd/4.0/>.

© The Author(s) 2025